

Quality of Service in aggregated quantum networks

Nicolo Lo Piparo,^{1,*} William J. Munro,^{1,2} and Kae Nemoto^{1,2}

¹*Okinawa Institute of Science and Technology Graduate University,
1919-1 Tancha, Onna-son, Okinawa, 904-0495, Japan.*

²*National Institute of Informatics, 2-1-2 Hitotsubashi, Chiyoda-ku, Tokyo 101-8430, Japan.*

Future quantum networks will enable the interconnection of multiple users distributed across vast geographic distances. Due to these large separations and limited physical resources, communication will often rely on multi-path routing strategies, where physical resources are distributed across channels of varying lengths and delivered to end users. Efficient long-distance quantum communication therefore requires optimizing the allocation of these resources across available paths. In this work, we introduce a performance-oriented approach to quantum network routing by extending the classical concept of Quality of Service (QoS) to the context of multi-path quantum resources distribution. Unlike prior models that consider entanglement generation or quantum memory coherence in isolation, we investigate the interplay between path assignment strategies, coherence time constraints, and quantum error correction (QEC), and how they jointly impact end-to-end communication fidelity. We analyze both unencoded and encoded transmissions over aggregated network paths, quantifying the effects of resource allocation on transmission success. Our findings show that fidelity cannot be optimized independently of memory lifetimes, and that while QEC can enhance performance under specific conditions, it also imposes additional constraints depending on network topology and path-length asymmetries. This work provides a foundation for developing QoS-aware quantum routing protocols that balance fidelity, throughput, and memory utilization—key considerations for near-term quantum repeater networks.

I. INTRODUCTION

Large-scale quantum networks aim to connect users distributed across geographically distant locations by establishing entangled quantum states between them [1–3]. Entanglement swapping operations at intermediate nodes will enable long-distance connections, ultimately contributing to the realization of a global quantum internet [4]. Such a network will offer fundamentally new capabilities, enabling users to harness quantum technologies that surpass the performance of classical systems. For example, connecting spatially separated quantum processors across the network could significantly enhance the computational power of distributed quantum computers [5–11]. Secure communication between remote users will also be made possible through quantum key distribution and related protocols [6, 12–15]. Moreover, linking multiple quantum sensors or clocks across nodes can boost the precision and accuracy of quantum metrology applications, such as clock synchronization and remote sensing [16–18].

Despite the profound differences between classical and quantum networks, many similarities remain—especially given that quantum networks will be deployed atop existing telecommunication infrastructure. In both cases, the number of physical resources available at each node is inherently limited, leading to potential congestion. This congestion can severely affect network performance by reducing data throughput or degrading the fidelity of quantum states.

In classical networks, congestion and resource contention are managed using a suite of traffic control techniques that collectively define Quality of Service (QoS) [19–21]. QoS metrics include bandwidth (data transfer rate), loss (fraction of lost data), delay (end-to-end transmission time), and jitter (variability in packet arrival times). These metrics guide network design and optimization to ensure that performance requirements are met even under constrained resources.

Similar considerations will be critical for the design of quantum networks. However, the extension of QoS concepts to the quantum domain must take into account fundamental physical differences. For instance, in a quantum network, delays often require temporary storage of quantum states in quantum memories, which are inherently susceptible to decoherence. This leads to fidelity loss—an effect absent in classical communication. As such, a quantum version of QoS must incorporate both conventional performance metrics and quantum-specific considerations such as memory coherence, noise, and quantum error correction (QEC) overhead.

Recent efforts have begun to formalize QoS in the quantum setting [22]. For example, Cicconetti et al. [23] explored how trade-offs between fidelity, latency, and throughput arise in realistic quantum architectures. Their work showed that multipath transmission can enhance network resource utilization, motivating our investigation of aggregated quantum networks (AQNs), in which quantum information is distributed over multiple paths to improve performance. In this work, we build upon that direction by introducing a QoS-aware channel assignment protocol for AQNs in a non-entanglement-based transmission model [24]. Unlike most prior studies that focus on entanglement distribution, swapping, or

* nicopale@gmail.com

purification [23, 25–27], our model is based on the direct transmission of quantum information—encoded or unencoded—through noisy channels. In this scenario, quantum error correction may be applied to protect the transmitted state from loss and noise [24, 28–34]. Interestingly, our analysis reveals that QEC does not always improve fidelity. In regimes with short coherence times or unbalanced path lengths, the overhead introduced by encoding can actually degrade the overall performance. This nontrivial result highlights the importance of developing integrated routing and encoding strategies that explicitly account for the physical limitations of hardware.

Here, we focus on key features of a quantum network that could pave the way for future in-depth investigations. Specifically, we consider a setting where two distant nodes, each hosting multiple users and a finite number of communication channels, aim to exchange quantum information with a target fidelity. While selecting fidelity as the primary figure of merit may appear restrictive, high-fidelity transmission is essential for realizing the advantages of quantum communication over classical methods. We model these two nodes as connected by multiple paths of varying lengths, each consisting of a series of lossy channels. To mitigate the effects of loss, we consider encoding the quantum state into a higher-dimensional system using QEC, distributing the encoded components across the available paths.

In AQNs, quantum packets (qubits or qudits) representing the encoded state are sent through different paths and later recombined at the receiver node for decoding. Thus, optimal channel assignment plays a crucial role in maintaining fidelity. We propose a routing protocol that distributes the encoded state across multiple channels in response to user demands, guided by QoS-inspired metrics tailored to the quantum setting. This framework allows us to define and optimize QoS parameters for AQNs, extending the classical concept into the quantum domain.

Importantly, our model departs from entanglement-based approaches. No entanglement generation, swapping, or purification steps are involved. Instead, we focus entirely on direct transmission of quantum information through noisy channels, a relevant model for near-term quantum networks constrained by hardware limitations.

This paper is organized as follows. In Sec. II, we define QoS metrics adapted to aggregated quantum networks. In Sec. III, we introduce a quantum router protocol for channel assignment based on these metrics. In Sec. IV, we present a case study illustrating how routing decisions impact fidelity under temporal delays and path asymmetries. Finally, we conclude in Sec. V.

II. QUALITY OF SERVICE OF AN AGGREGATED QUANTUM NETWORK

We now extend the QoS concepts introduced earlier to the context of an Aggregated Quantum Network

(AQN), beginning with some basic definitions. It is important to emphasize that our model does not rely on entanglement-based primitives. As a result, phenomena such as stochastic link establishment arising from probabilistic entanglement swapping—which are central to repeater-based architectures—are not relevant in our setting. Instead, we consider a direct transmission model in which quantum states are sent over lossy channels characterized by fixed or known delays. In general, the network can be represented as a graph, where nodes (vertices) are connected by communication links (edges), as illustrated in Fig. 1. We will refer to the vertices of a quantum net-

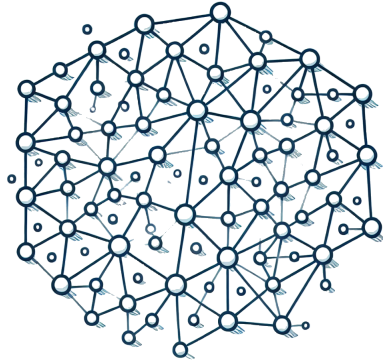


Figure 1. A generic quantum network represented by a set of vertices (nodes) connected by edges (links). Each link can contain multiple channels. The set of links that connects two nodes is a path.

work as *nodes* and to the edges connecting them as *links*. A *link* represents either a physical or logical connection between two nodes, while a *channel* denotes the specific transmission medium—physical or logical—used to carry quantum information. More precisely, a channel may correspond to a dedicated physical medium, such as an optical fiber or free-space optical connection, or to a logical subdivision within a multiplexed medium. Since a link may support multiple channels, we define the *capacity* of a link as the aggregate capacity of all channels associated with it. A *path* is the sequence of links and intermediate devices that a quantum packet traverses en route from source to destination. The length of a path, denoted by L , is the sum of the lengths of its constituent links and is measured in kilometers. In AQNs, quantum information is distributed across multiple parallel paths—each potentially of different length—that collectively connect a sender to a receiver. This set of paths constitutes an aggregated path. In such a scenario, several QoS metrics must be redefined or adapted to account for the unique features of AQNs.

- **Bandwidth:** the bandwidth of a single path is determined by the capacity of the bottleneck link—i.e., the link along the path with the lowest capacity. For an aggregated path, the bandwidth is defined

as the sum of the capacities of all constituent paths. Bandwidth thus quantifies the maximum amount of information that can be transmitted across the path per unit time, providing users with an estimate of the available data rate.

- **Loss:** the loss of information transmitted across noisy channels can be measured in several ways. We adopt the infidelity of the transmitted state, $1 - F$, where F is the fidelity of the state received and processed at the receiver's node. The infidelity might depend on several errors, such as the channel loss, parametrized by the transmission coefficient $p = \eta e^{-L/L_{att}}$, where L_{att} is the attenuation length that depends on the type of channel in use, and η is a loss term due to interactions with other components of the network, such as quantum memories (QMs) and frequency converters. In an aggregated quantum network the infidelity depends also on the decoherence time of the QMs used to store the quantum states at the receiver's node [35].
- **Delay:** the *delay*, τ_P , of a path is defined as the time interval between the time the quantum data packets are sent by the sender node and the time they arrive at the receiver node. It is given by $\tau_P = L/c + t_c$, where L is the length of the path, c is the speed of light traveling in the medium (optical fiber or free space) while t_c is the congestion time. The latter is the extra time due to the waiting time some packets might require at the intermediate nodes and the processing time. In fact, one can think that when the physical resources travel across multiple nodes before reaching the far end, some of those intermediate nodes might be not be immediately accessible or could take some time to process the quantum data packet. Therefore, some delay line must be added before the resources can pass through that node. This time can be then considered as the sum of all those extra delays. This definition of delay can be generalized by including more temporal terms due to the queuing times. The congestion time is, therefore, dynamic and dependent on queuing and processing times. [36].
- **Jitter:** this is defined as the time difference of the arrival times of the information packets. Whereas in classical networks such a time difference will cause a delay in the information flow, in aggregated quantum networks that information must be stored into QMs. Therefore, the stored states will undergo a depolarization/dephasing process that will deteriorate the fidelity of the final state, resulting in a loss of information. Here we have assumed the jitter is negligible. However, in a real implementation the jitter can be different from zero and, in this case, must be considered.

In the quantum networking regime, these metrics can overlap. For instance in some models, particularly

those involving entanglement distribution or application-specific fidelity guarantees, it may be useful to define an ‘effective bandwidth’ that combines channel capacity with a minimum required fidelity. However, in our work, we do not impose such constraints. Our model evaluates the actual fidelity achieved under different channel assignments but does not enforce a fidelity threshold. As a result, bandwidth and loss are treated as separate performance metrics in the unencoded case. In the encoded case, they may become indirectly related via the redundancy of the quantum error correction code, but we do not introduce an explicit effective bandwidth definition. Based on the above quantum network definitions of QoS, we can now qualitatively estimate the requirements of a few quantum protocols, as shown in the radar plot of Fig. 2. In a conventional quantum key distribution (QKD)

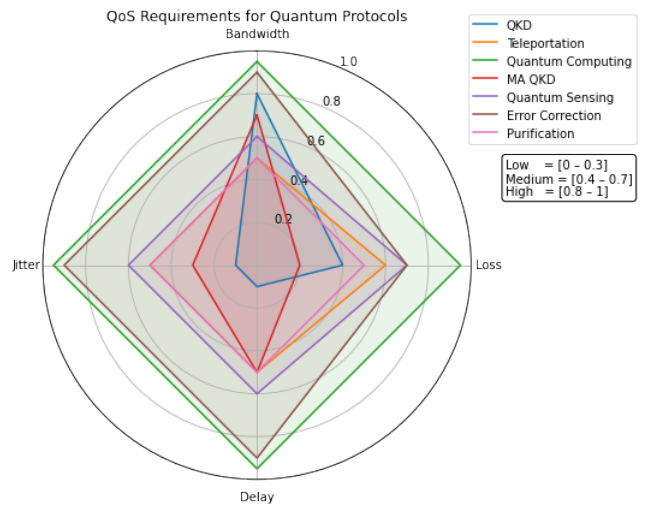


Figure 2. The chart provides a qualitative comparison of the performance requirements of various applications across key QoS metrics. The normalized values are not drawn from experimental data but are instead intended to illustrate conceptual differences among protocols, helping guide the design of routing strategies suited to specific use cases. The range of normalized values for “low”, “medium” and “high” requirements is in the box below the legend.

protocol the rate at which two users can share a secret key is the main figure of merit. Therefore, the bandwidth plays a fundamental role and it must be high [37]. Similarly, for distributing quantum computing high bandwidth is necessary to connect multiple nodes faster [38]. For memory assisted (MA) QKD and conventional purification protocols the bandwidth can be slightly lower, as quantum memories store the quantum states increasing the probability of successfully sharing information [39]. Also, for quantum remote sensing, we need to generate complex states like GHZ states, which need higher quality (fidelity) [40]. A lower bandwidth is required for quantum teleportation since a single entangled state is sufficient for its realization. Then, a small delay and the jitter for QKD protocols do not affect the efficiency of

these systems since a delayed secret key and an irregular transmission of the arriving packets do not compromise the security of the shared key. A medium requirement on both the delay and jitter is, on the other hand, needed for purification, teleportation and remote sensing as storing entangled states might affect the quality of the final states due to decoherence processes in the QMs. Distributing quantum computing is highly affected by delay and jitter as it is fundamental that the packets arrive regularly and at precise times at each node to be processed correctly. Finally, the loss of information has a low impact on a MA-QKD protocol because the states are stored into QMs before extracting a secret key. This loss has a medium effect on conventional QKD systems as it might reduce the secret key rate. Analogously for purification the loss of information has a medium impact on the efficiency of this protocol because several entangled states need to be created to increase the fidelity of the final state. Then, for distributing quantum computation the quantum error correction codes in use can restore the loss of information with some probability, having, thus, a medium impact on these systems. On the contrary, losses have a more detrimental effect on the sensitivity of a sensing protocol and can move us away from the Heisenberg limit [41]. This is especially true as the kind of resource states we are generating can be completely destroying if a single qubit it loss.

Figure 2 presents a radar chart summarizing the QoS requirements of various quantum applications. These requirements exhibit diverse performance profiles: some applications demand high fidelity, while others are more tolerant of latency or jitter. Notably, the chart illustrates that no single routing policy can optimally satisfy all applications simultaneously—particularly in networks with limited bandwidth or highly variable channel quality across different paths. This observation raises a fundamental design challenge for near-term quantum networks: how should a router allocate transmission resources—such as quantum channels along multiple paths—to meet the potentially conflicting QoS demands of multiple users? In the following section, we address this question by introducing a time-slotted quantum router model and analyzing several channel assignment strategies under resource-constrained conditions.

III. THE ROUTING PROTOCOL

We consider a scenario in which multiple users issue requests to transmit quantum information—using either qubits or qudits—over a quantum network composed of multiple transmission paths and coordinated by a quantum router. The router is responsible for assigning available quantum channels to these requests in a manner that satisfies or balances relevant Quality of Service (QoS) metrics. Our model adopts a time-slotted structure, in which time is divided into discrete, fixed-duration intervals (slots). Each slot corresponds to the transmission

window of a quantum “packet,” defined here as a group of qudits sent from a user to a destination node.

All slots are assumed to have equal duration, determined by the time required to transmit a single packet (i.e., a batch of qudits). We do not assume global synchronization across the entire network, as this would require impractically precise timing mechanisms. Instead, we assume local synchronization between directly connected nodes, which is consistent with the capabilities of current quantum key distribution (QKD) systems, where local time alignment can be achieved via classical signaling or embedded timing protocols [42, 43].

The quantum router does not directly transmit quantum information but acts as a decision-making component that allocates quantum channels and manages resource assignment across the network. It interfaces with underlying quantum switches, which are responsible for the physical transmission of qudits. The router performs higher-level control functions, including receiving user requests (e.g., the number of qudits to be sent), querying or maintaining the current state of each transmission path (such as channel availability and estimated loss or delay), and assigning channels to users according to a specified routing policy.

By contrast, quantum switches operate at the physical layer, forwarding qudits based on the router’s assignments. Routers and switches exchange control information over a classical control channel, in line with standard practices in quantum network control architectures [44]. Users communicate with the quantum router via a classical interface, specifying the destination node, the number of qudits to transmit, and optionally a QoS preference.

In our model, we assume that the quantum router has knowledge of the following:

- The number of available channels along each path,
- The estimated delay and length of each path (which affect fidelity and timing),
- The coherence time of the quantum memories at the destination node, used to determine whether the qudits will survive the full transmission time,
- The set of current user requests.

The router does not perform entanglement distribution, purification, or entanglement swapping. Instead, our model focuses on the direct transmission of quantum information, where quantum memories serve primarily as buffers to temporarily store qudits until transmission can be completed. This architectural choice enables the router to reject or reroute requests whose expected delay exceeds the coherence time of the available memory, as illustrated in the examples presented in Sec. IV.

A. Routing protocol description

Let us now describe our routing protocol for a simple wide area network (WAN) as illustrated in Fig. 3. We

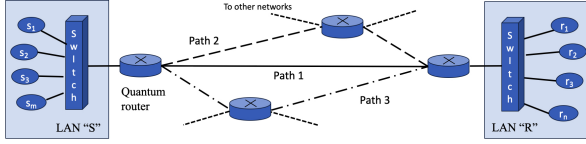


Figure 3. Schematic illustration of a wide-area quantum network (WAN) with quantum routers. Two local area networks (LANs), labeled “S” (source) and LAN “R” (receiver), are connected via three distinct paths: a solid line (path 1), dashed lines (path 2), and dash-dotted lines (path 3). These paths differ in length and may each contain an arbitrary number of quantum channels, over which information can be transmitted from LAN S to LAN R. A quantum router assigns available channels for transmitting quantum packets according to a specified operational policy based on user requests, or it may deny requests if network resources are insufficient to meet the stated requirements. Each path may also include intermediate routers that connect to other networks.

consider two local area networks (LANs), denoted LAN “S” (source) and LAN “R” (receiver), containing m and n users, respectively. Both LANs are connected to quantum routers, which are, in turn, linked via multiple paths of varying delay. Each path may include an arbitrary number of quantum channels over which information is transmitted. While a real-world quantum network may support many such paths between distant LANs, for illustrative purposes Fig. 3 depicts three representative paths: a solid line (path 1), dashed lines (path 2), and dash-dotted lines (path 3).

The objective is to allocate the available resources in LAN “S” across the various channels connecting it to LAN “R.” To this end, we envision a routing mechanism that follows a multi-step protocol. Initially, users in LAN “S” issue requests to communicate with users in LAN “R,” specifying desired performance criteria—such as a minimum threshold fidelity for received quantum information or a target transmission rate (request step). The quantum router then evaluates whether the available resources in both LANs are sufficient to fulfill these requirements (processing step).

If a request cannot be satisfied with the current resource state, the router temporarily queues it for a fixed number of time steps. If the network lacks the capacity to meet the request even under future conditions, the router issues a denial signal, notifying the user that the communication cannot proceed and awaits the next input. Otherwise, the router proceeds to the assignment step, in which it distributes available resources across the selected channels. We now examine each of these steps in more detail.

B. Request step

In the request step, the primary figure of merit is evaluated. Upon receiving an input request, the quantum router first determines whether error protection is required to guarantee the desired fidelity (if that is the desired metric) of the transmitted quantum state. If error protection is necessary, the router then identifies the appropriate operational regime. Multiple regimes may be considered depending on user requirements. For example, the router might prioritize a single user or a small subset of users, thereby limiting access to the transmission paths for the majority. Alternatively, it may ensure that most users gain access to the available paths. While numerous scenarios are possible, in the following section we focus on three representative regimes, leaving a more comprehensive analysis for future work.

Once the request step is completed, the router proceeds to the processing step. Here, it analyzes the available resources in LAN “S,” the coherence times of quantum memories in LAN “R,” and the characteristics of the connecting paths. Based on this information and the selected operational regime, the router assigns channels to the users in LAN “S.” This step is critical for optimizing protocol performance, and we provide a simple illustrative example in the next section.

Finally, after processing, the quantum router instructs the switch device to establish connections for users to transmit their data. The router then resets and initializes for the next operational cycle.

IV. ROUTING ASSIGNMENT IN THE UNENCODED SCENARIO

Selecting an appropriate channel assignment can enhance network performance. Quality of Service (QoS) features inform this selection; here, we focus on two key aspects: bandwidth and loss. We assume that channels have limited capacity and that information may be lost during transmission or degraded when stored in quantum memories (QMs). In this section, we present an example illustrating how a router can assign multiple channels between two distant nodes, S and R, each hosting a variable number of users seeking to exchange information. We assume that S and R are connected by N_c channels with $N_c/2$ channels contained into a path with delay τ_1 and the remaining $N_c/2$ channels in a path with delay $\tau_2 > \tau_1$. Let us further assume that a router at node S assigns channels to users, across which they transmit their quantum states to node R. A natural question then arises: what is the optimal channel assignment? To answer this question we can explore three possible scenarios. In scenario (a), called the *greedy regime*, a single user maximizes the quality (fidelity) of their transmitted state. In scenario (b), the goal is to satisfy the requirements of as many users as possible (*balanced regime*). In scenario (c), a limited number of users aim to maxi-

Assignment 1		Assignment 2		N_u
path 1	path 2	path 1	path 2	
5	0	0	5	2
4	1	1	4	2
3	2	2	3	2
5	5	5	5	4

Table I. Assignments of the number of qudits transmitted along two paths in the unencoded scenario. Each row corresponds to a possible channel assignment among N_u users. Configurations highlighted in blue are affected by decoherence occurring in the quantum memories (QMs) located at node R. These QMs store packets that arrive earlier, holding the quantum states until the packets traveling through the longer-delay path are ready to be processed.

mize their fidelities, subject to the condition that the differences among them remain small (*restricted regime*). Depending on the selected regime the router will assign the available channels accordingly. The question now is: what is the optimal assignment strategy in each of the three regimes? In this Section we show with an example what is the best assignment when users send information using five packets. Consider that $N_c = 10$ and that the capacity of each channel can transmit a qudit of dimension 9 per time unit. A user could send a single lower-dimensional qudit or, alternatively, two qudits of dimension 3 (qutrits). For simplicity, let us assume that $\eta_1 = \eta_2 = 1$ and $t_{c1} = t_{c2} = 0$. Table I presents all the possible assignments of the channels of path 1 and path 2 among N_u users, with N_u being the highest number of users that can be served given the above conditions. For instance, the first line of table I gives the number of qudits traveling in each path for two assignments given to two users. In this case, under assignment 1, one user transmits a packet of five qudits of dimension 7 through the channels along path 1, while another user sends their five qudits of the same dimension through the channels of path 2. This configuration corresponds to the greedy regime, in which the router assigns the lowest-loss channels to a single user, leaving the remaining channels (in path 2) to the other user. Consequently, the fidelity of the "greedy" user reaches the maximum achievable with the available resources, assuming $p_1 = 0.95$ and no decoherence, as shown by the solid line in Fig. 4. In contrast, the fidelity of the packets sent by the other user is the lowest, as indicated by the cross symbols in Fig. 4. Next, in the restricted regime, the router assigns channels to users with the goal of minimizing the difference between their fidelities. This condition is satisfied by the configurations represented by the dotted and dash-dotted lines in Fig. 4. The balanced regime, in this case, corresponds to one of the three configurations listed in Table I, since the maximum number of users that can utilize the network is two. The mathematical expressions for the fidelities shown in Fig. 4 are provided in Appendix A.

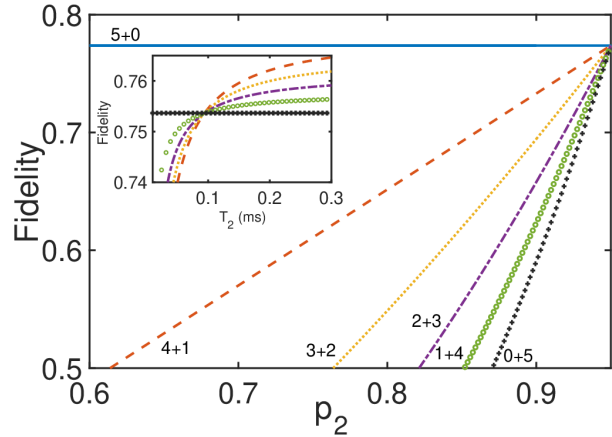


Figure 4. Fidelities of the received packets at the receiver node as a function of the transmission probability of path 2, p_2 , corresponding to qudit assignments listed in Table I with $p_1 = 0.9$ and $T_2 \rightarrow \infty$. The label of each curve refers to the number of qudits sent through path 1 and path 2, corresponding to the assignments of Table I. The inset depicts the fidelities of the packets at the receiver node versus the coherence time, T_2 , for $p_1 = 0.95$ and $p_2 = 0.945$.

It is now interesting to see the effects of a finite coherence time in such a scenario. The configurations, highlighted in blue in Table I, require quantum memories at the receiver's node due to the fact that the paths have different delay (length in this case) and, therefore, the receiver node must store the quantum states arriving earlier before the total packet can be processed. However, at low coherence times, the decoherence might affect a configuration with the majority of the qudits traveling in the shorter path much more than a configuration with a larger number of qudits traveling in the longer path, as shown in the inset of Fig. 4. One can see that at $T_2 < 0.1$ ms and at $p_2 = 0.945$ the fidelity of the transmitted packet corresponding to the assignment 4+1 (3+2) is higher than the fidelity corresponding to the assignment 1+4 (2+3). For these configurations it is then fundamental that the router is informed with the coherence time of the QMs at the receiver node to optimally assign the channels to the users. Remarkably, the inset shows that the fidelities of those configurations all cross with the 0+5 configuration at $T_2^\dagger = 0.1$ ms. This means that for $T_2 < T_2^\dagger$ the aggregation scenario is not convenient for a possible router's assignment. Finally, the regimes defined above are not affected by finite coherence times.

V. ROUTING ASSIGNMENT IN THE ENCODED SCENARIO

In this section, we illustrate, via an example, how a router assigns the channels between two nodes by selecting between a conventional network where the informa-

tion is encoded and transmitted across one or multiple paths with different delays. For those different scenarios we compare the fidelities with the analytical formulas obtained in [35]. We denote with “ F_{i+j} ” the fidelity of the configuration $i + j$ in which i (j) qudits have been transmitted across the first (second) path.

Let us consider two distant nodes, S and R, exchanging information using the quantum Reed-Solomon (QRS) code [45] in a quantum aggregation scenario. Similarly to the unencoded case, we assume here that the number of users in S is a variable and node S and R are connected by path 1 and path 2. For a fixed transmission probability p_1 of the channels in path 1, the best assignment depends on the transmission probability of the channels in path 2 and on the coherence time of the QMs at node R. Let us illustrate the answer to this question with a simple example. Consider that $N_c = 10$ and the capacity of each channel can transmit a qudit of dimension 9 per time unit. For simplicity, we also assume that $\eta_1 = \eta_2 = 1$ and $t_{c1} = t_{c2} = 0$. Now, each row of Table II contains the number of qudits that can be sent per path with the above conditions (highest capacity of the channel and number of channels per path). For instance, in the first row of Assignment 1, a single user encodes their information with a 7 dimensional QRS code, with 5(2) qudits of dimension 7 traveling in path 1(2), respectively. Assignment 2 allows two users to encode their information with a 3 dimensional QRS code by sending 3 qutrits across path 2. In this case, the highest capacity have been achieved by the transmitted qudits therefore no more assignments are possible (i.e., 0 qudits in Assignment 3). On the contrary, the eighth row of Table II shows that, when all users are encoding their state with a 3-dimensional QRS code, three Assignments are possible. In Assignment 1 two users are sending their three qutrits on path 1, two users send one qutrit on path 1 and two qutrits on path 2 in Assignment 2, and other two users send three qutrits on path 2 in Assignment 3. The last column of Table II contains the highest number of users, N_u , that can be served given the above conditions. We define the degeneracy of an assignment as the highest number of users that can encode their state with the quantum packets of that specific assignment. In the example above, for the first row of Table II the degeneracy of Assignment 1 is one whereas the degeneracy of Assignment 2 is two as two users can encode their state with a 3 dimensional QRS code. For simplicity, for the assignment i ($i \in \mathbb{N}^*$) with degeneracy higher than one we refer to user i as a single user that represents that assignment.

Now we analyze in more detail the various assignments and the regimes with which they can be associated. Firstly, due to the different lengths of the two paths some assignments (blue lines in the table) might be affected by a temporal delay as shown in [35]. This can significantly change the resulting fidelity depending on the coherence time, T_2 , of the quantum memories in use. Another factor to consider is the length of path 2. Let us begin

Assignment 1		Assignment 2		Assignment 3		N_u
path 1	path 2	path 1	path 2	path 1	path 2	
5	2	0	3	0	0	3
4	3	1	2	0	0	3
3	4	2	1	0	0	3
2	5	3	0	0	0	3
5	0	0	5	0	0	2
4	1	1	4	0	0	2
3	2	2	3	0	0	2
3	0	2	1	0	3	6
3	0	1	2	1	2	6
2	1	2	1	1	2	6
				1	2	6
				1	2	6

Table II. Assignments of the number of qudits traveling along two paths in the aggregation scenario. Each row corresponds to a possible assignment of channels among N_u users. Configurations affected by decoherence in the quantum memories (QMs) located at node R are highlighted in blue. The QMs are needed when the number of qudits arriving at R via the shorter path is not sufficient to decode the state. The dimension of the qudits used is constrained by the total capacity of each path.

our analysis with the asymptotic case $T_2 \rightarrow \infty$ (ideal memories). Figure 5(a) shows the fidelities of the transmitted states of user 1 and user 2, respectively, for the first four configurations of Table II. Here the curves of the same colors correspond to the fidelities of each single row and the solid (dashed) curves represent the fidelities of the transmitted states of user 1 (2), respectively, for a transmission coefficient of path 1 $p_1 = 0.9$. One can see that, when more qudits are traveling in the shorter channel (red and blue curves), user 1 consistently achieves higher fidelities than user 2. In contrast, when more qudits travel along path 2 (purple and yellow curves), the advantage for user 1 occurs only for certain values of p_2 (crossing points between curves of the same color). This behavior can be explained by the fact that in the aggregation scenario the fidelities of the configurations most packets travel through the longer channels strongly depend on the length of that path. The crossing points of Fig. 5(a) can be used to determine the optimal distribution of quantum packets in the restricted regime, where the goal is to minimize the fidelity difference between users.

Next Fig. 5(b) shows the fidelities of the transmitted states for the corresponding configurations of Table II. Here, the curves do not cross because both users send the same number of qudits, although user 1 utilizes more channels in the shorter path than user 2. The results in Fig. 5(b) can be used for the greedy regime by selecting the communication path with the highest fidelity and for the restricted regime by analyzing the plot of the difference of the fidelities. For simplicity, to determine the optimal configuration for the restricted regime we plot in Figure 6 only the difference of the fidelities of the

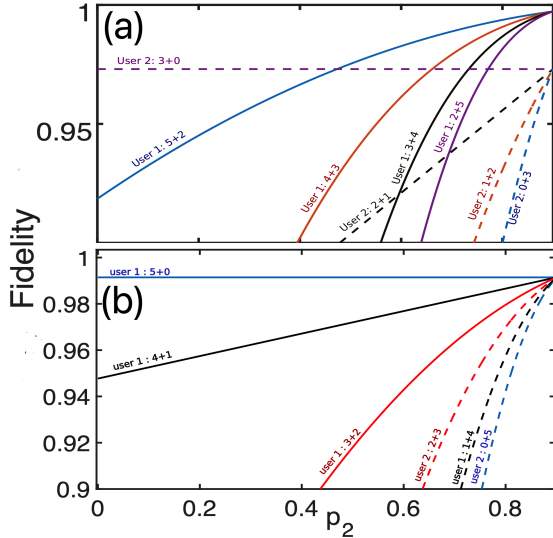


Figure 5. Fidelities of the decoded states at the receiver node versus the transmission probability of path 2, p_2 , corresponding to the qudit assignments of Table II, with $p_1 = 0.9$ and $T_2 \rightarrow \infty$. Curves of the same color correspond to each row in Table II. Solid (dashed) curves refer to user 1 (2), respectively. The fidelities in (a) can be used to identify the greedy regime—since some configurations employ the highest qudit dimension—the restricted regime—because some fidelity curves intersect, thereby minimizing their difference—and the balanced regime—due to configurations involving the lowest number of qudits. Panel (b) shows fidelities relevant for identifying both the restricted and greedy regimes. Specifically, the restricted regime includes configurations with closely matching fidelities, while the greedy regime includes configurations whose performance is independent of the coherence time.

transmitted states of user 1 and user 2 of the $3+2$ and $2+3$ configuration (red curve), $4+3$ and $1+2$ configuration (blue curve) and $3+4$ and $2+1$ configuration (black curve) versus p_2 . As one can see the graph can be divided into three parts for certain range of p_2 . Specifically, for $0.65 < p_2 < 0.71$, the configurations that minimize the difference between the fidelities of user 1 and user 2 correspond to distributing the resource according to $3+2$ the configuration for user 1 and $2+3$ for user 2 (red curve). Next, for $0.71 < p_2 < 0.8$, the black curve minimizes the difference of the fidelities corresponding to the $3+4$ configuration for user 1 and $2+1$ for user 2. Finally at $p_2 > 0.8$ the smallest difference of fidelities is given by the $4+3$ configuration for user 1 and $1+2$ configuration for user 2.

Further, the fidelities of the balanced regime corresponding correspond to the communication paths in the last three rows of table II. Given the available resources, up to 6 users can be served, as each assignment has a degeneracy of 2. Even for this regime subcases may arise in which users might want to minimize the difference in their fidelities (fair balanced regime) or assign most of the resources traveling through the shorter channel to

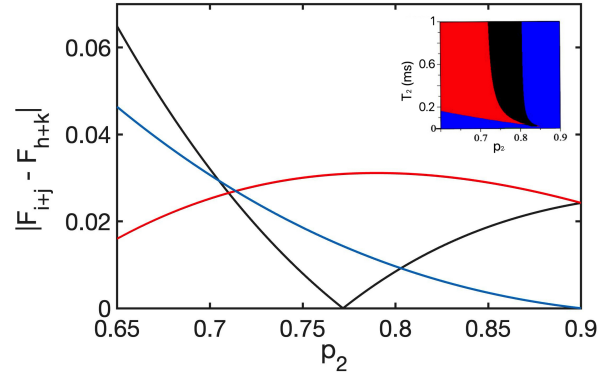


Figure 6. Absolute value of the difference between the fidelities of the transmitted states, where i, j, k and l correspond to the following configurations: $3+4$ and $2+1$ (red curve), $3+2$ and $2+3$ (blue curve), and $2+5$ and $3+0$ (black curve). In the restricted regime, the router assigns the $3+4$ and $2+1$ configuration (red curve) for $0.65 < p_2 < 0.71$, the $2+5$ and $3+0$ configuration (black curve) for $0.71 < p_2 < 0.81$, and the $4+3$ and $1+2$ configuration (blue curve) for $p_2 > 0.81$. The inset shows the optimal configurations when fidelities are affected by the coherence time T_2 , by plotting T_2 versus p_2 .

one user (unfair balanced regime).

Next we consider the case in which the router selects the best configuration in the greedy regime. For instance, if user 1 requires the highest fidelity, the router will assign user 1 most of the resources traveling along path 1. To this end we then compare the fidelity of the configuration $5+2$ with the fidelity of the configuration $5+0$ as shown in Fig. 7. Interestingly, the advantage of using

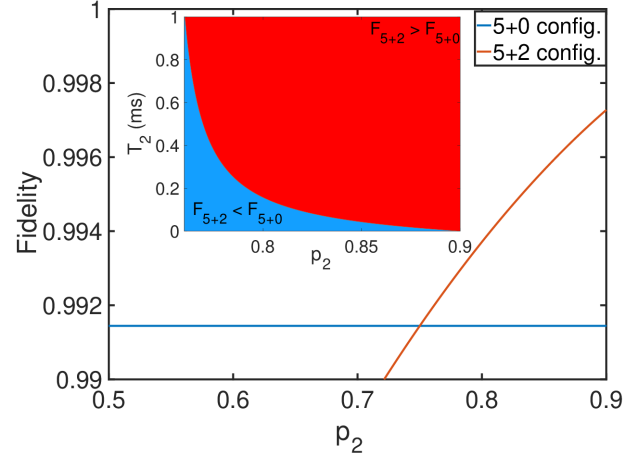


Figure 7. Fidelity of the transmitted state corresponding to the $5+2$ configuration (red curve) and $5+0$ configuration (blue line). The inset shows the optimal configurations when the fidelities are affected by the coherence time, T_2 , by plotting T_2 versus p_2 .

higher dimensional code is achieved for $p_2 > 0.75$. For lower values of p_2 it is more advantageous to encode the state in a lower dimensional code. This might seem a bit

counterintuitive because the 7-dimensional QRS code can tolerate the loss of three qudits while the 5-dimensional code can tolerate the loss of only 2 qudits. Therefore, one might think that at $p_2 = 0$, i.e., when the two qudits traveling in path 2 are lost, the fidelity of the encoded state using the 7-dimensional code is equal to the fidelity of the 5 dimensional code. This not the case, because when the two qudits in path 2 are lost the 7-dimensional code can tolerate the loss of one qudit traveling in path 1 (or, obviously, zero qudit). Therefore the contribution to the fidelity in this case are proportional to p_1^5 (no loss in path 1) and $p_1^4(1-p_1)$ (1 qudit loss in path 1). On the other hand, when the state has been encoded with a 5-dimensional QRS code with all qudits traveling in path 1, the fidelity will also have a contribution proportional to $p_1^3(1-p_1)^2$ in addition to the above contributions. These results are obtained for ideal QMs at the receiver's node, in which the coherence time is assumed to be infinite.

A. The effect of finite coherence of QMs

Let us now consider the case in which the QMs at the receiver's node are not perfect and have a finite coherence time T_2 . This can drastically change the optimal assignment made by the router as illustrated in the following example. Let us assume we are in the greedy regime, in which a single user demands that its transmitted state achieves the highest possible fidelity with the available resources. Looking at Fig. 7 one notices that at $p_2 < 0.72$ the 5+0 configuration is the most advantageous. We want to determine then for which values of T_2 the 5+2 configuration has a better performance than the 5+0 configuration for $p_2 > 0.75$. The inset of fig. 7 shows the red(blue) area delimited by the coherence time T_2 and by p_2 to obtain a fidelity of the transmitted state higher(lower) in the 5+2 configuration compared to the 5+0 configuration. For $T_2 > 1$ ms the asymptotic regime is achieved and the coherence time only slightly affects the fidelity in the 5+2 configuration. However, for $T_2 < 1$ ms one can see that higher values of p_2 are needed to guarantee that the 5+2 configuration gives an advantage compared to the 5+0 configuration.

Similarly the inset of Fig. 6 shows that the coherence time plays a relevant role in assigning the channels in the restricted regime as well. First one can notice that at $T_2 = 1$ ms the asymptotic regime is achieved as well as in the greedy regime. Next, at lower values of $T_2 > 0.2$ ms, the 3+4 and 2+1 configurations (red area) have more similar fidelities than the 2+5 and 3+0 configuration (black area). It is noteworthy to notice that at $T_2 < 0.2$ ms the 3+2 and 2+3 have much more similar fidelities than all the other configurations under consideration.

These results highlight that coherence time can play a critical role in determining the optimal assignment of

channels. Therefore, it is essential that the router be informed of the coherence time of the QMs used at the remote end to ensure it meets the users' performance expectations.

VI. CONCLUSION

In this work, we have introduced the concept of Quality of Service (QoS) tailored for quantum and aggregated quantum networks, providing a qualitative description of their requirements across several quantum communication applications. We proposed a routing protocol for the optimal assignment of quantum channels connecting two remote nodes with multiple users, illustrating its effectiveness through two representative scenarios.

Our analysis showed that when users transmit unencoded quantum states, the coherence time of quantum memories does not impact optimal channel assignment within the considered regimes, though a threshold coherence time exists below which quantum aggregation is no longer advantageous. In contrast, when employing quantum error correction—specifically, the quantum Reed-Solomon code—the optimal assignments strongly depend on both channel transmission probabilities and the coherence times of quantum memories at the receiver node. We quantified coherence time thresholds above which decoherence effects become negligible, demonstrating that current quantum memory technologies, such as ion qubits, superconducting cavities, and ensemble-based systems, are suitable for such networks.

Although our model focuses on quantum networks without entanglement distribution, it draws inspiration from classical wireless mesh networks [46, 47], leveraging concepts like decentralized routing, multi-user coordination, and QoS-aware path selection to guide protocol design. We identified bandwidth and loss as crucial QoS parameters for optimizing channel assignment in small-scale aggregated networks, and suggest that incorporating additional metrics such as delay and jitter could further improve performance.

Overall, this work establishes QoS as a vital figure of merit for quantum networks and provides a foundation for optimizing their design and operation in future implementations.

ACKNOWLEDGMENTS

We thank Mohsen Razavi for the interesting discussion. This project was made possible through the support of the Moonshot R&D Program Grants JPMJMS2061 & JPMJMS226C, JSPS KAKENHI Grant Nos. 21H04880 and 24K07485.

[1] W. Kozlowski and S. Wehner, Towards large-scale quantum networks, In Proceedings of the 6th ACM International Conference on Nanoscale Computing and Communication (2019).

[2] L. Childress and R. Hanson, Diamond nv centers for quantum computing and quantum networks, MRS Bulletin **38**, 134 (2013).

[3] M. S. Blok, N. Kalb, A. Reiserer, T. H. Taminiau, and R. Hanson, Towards quantum networks of single spins: analysis of a quantum memory with an optical interface in diamond, Faraday Discuss. **184**, 173 (2015).

[4] H. J. Kimble, The quantum internet, Nature **453**, 1023 (2008).

[5] F. Arute, K. Arya, R. Babbush, D. Bacon, J. C. Bardin, R. Barends, R. Biswas, S. Boixo, F. G. S. L. Brandao, D. A. Buell, B. Burkett, Y. Chen, Z. Chen, B. Chiaro, R. Collins, W. Courtney, A. Dunsworth, E. Farhi, B. Foxen, A. Fowler, C. Gidney, M. Giustina, R. Graff, K. Guerin, S. Habegger, M. P. Harrigan, M. J. Hartmann, A. Ho, M. Hoffmann, T. Huang, T. S. Humble, S. V. I., E. Jeffrey, Z. Jiang, D. Kafri, K. Kechedzhi, J. Kelly, P. V. Klimov, S. Knysh, A. Korotkov, F. Kostritsa, D. Landhuis, M. Lindmark, E. Lucero, D. Lyakh, S. Mandrà, J. R. McClean, M. McEwen, A. Megrant, X. Mi, K. Michielsen, M. Mohseni, J. Mutus, O. Naaman, M. Neeley, C. Neill, M. Y. Niu, E. Ostby, A. Petukhov, J. C. Platt, C. Quintana, E. G. Rieffel, P. Roushan, N. C. Rubin, D. Sank, K. J. Satzinger, V. Smelyanskiy, K. J. Sung, M. D. Trevithick, A. Vainsencher, B. Villalonga, T. White, Z. J. Yao, P. Yeh, A. Zalcman, H. Neven, and J. M. Martinis, Quantum supremacy using a programmable superconducting processor, Nature **574**, 505 (2019).

[6] W. J. Munro, K. Azuma, K. Tamaki, and K. Nemoto, Inside quantum repeaters, IEEE Journal of Selected Topics in Quantum Electronics **21**, 6400813 (2015).

[7] M. Nielsen and I. Chuang, *Quantum Computation and Quantum Information* (Cambridge University Press, Cambridge, 2000).

[8] C. Bennett and D. DiVincenzo, Quantum information and computation, Nature **404**, 247 (2000).

[9] R. Raussendorf and H. J. Briegel, A one-way quantum computer, Phys. Rev. Lett. **86**, 5188 (2001).

[10] E. Knill, Quantum computing with realistically noisy devices, Nature **434**, 39 (2005).

[11] L.-M. Duan and R. Raussendorf, Scalable photonic quantum computation through cavity-assisted interactions, Phys. Rev. Lett. **95**, 080503 (2005).

[12] W.-Y. Hwang, Quantum key distribution with high loss: Toward global secure communication, Phys. Rev. Lett. **91**, 057901 (2003).

[13] A. K. Ekert, Quantum cryptography based on bell's theorem, Phys. Rev. Lett. **67**, 661 (1991).

[14] J. Qiu, Quantum communications leap out of the lab, Nature **508**, 441 (2014).

[15] D. Bunandar, A. Lentine, C. Lee, H. Cai, C. M. Long, N. Boynton, N. Martinez, C. DeRose, C. Chen, M. Grein, D. Trotter, A. Starbuck, A. Pomerene, S. Hamilton, F. N. C. Wong, R. Camacho, P. Davids, J. Urayama, and D. Englund, Metropolitan quantum key distribution with silicon photonics, Phys. Rev. X **8**, 12 (2018).

[16] D. S. Simon, G. Jaeger, and A. V. Sergienko, Quantum metrology, imaging, and communication book, Int. J. Quantum Inform. **12**, 1430004 (2014).

[17] L. A. Lugiato, A. Gatti, and E. Brambilla, Quantum imaging, J. Opt. B **4**, 176 (2002).

[18] C. L. Dogen, F. Reinhard, and P. Cappellaro, Quantum sensing, Rev. Mod. Phys. **89**, 035002 (2017).

[19] M. Fanizza, F. Kianvash, and V. Giovannetti, Quantum flags and new bounds on the quantum capacity of the depolarizing channel, Phys. Rev. Lett. **125**, 020503 (2020).

[20] M. Rosati, A. Mari, and V. Giovannetti, Narrow bounds for the quantum capacity of thermal attenuators, Nat. Commun. **9**, 4339 (2018).

[21] M. E. Shirokov, Uniform continuity bounds for characteristics of multipartite quantum systems, Journal of Mathematical Physics **58**, 102202 (2017).

[22] M. Skrzypczyk and S. Wehner, An architecture for meeting quality-of-service requirements in multi-user quantum networks, arXiv:2111.13124 (2021).

[23] C. Cicconetti, M. Conti, and A. Passarella, Quality of service in quantum networks, IEEE Network **36**, 24 (2022).

[24] W. J. Munro, A. M. Stephens, S. J. Devitt, K. A. Harrison, and K. Nemoto, Quantum communication without the necessity of quantum memories, Nature Photonics **6**, 777 (2012).

[25] A. Abana, M. Cubeddu, V. S. Man, and A. Battou, Entanglement routing in quantum networks: A comprehensive survey, arXiv:2408.01234 (2024).

[26] J. Li, M. Wang, Q. jia, K. Sue, N. Yu, Q. Sun, and J. Lu, Fidelity-guarantee entanglement routing in quantum networks, arXiv:2111.07764v4 (2022).

[27] K. Li, V. Chaudhary, S. Sanchez Garcia, and K. R. Chowdhury, Q-firm: Fidelity-based rate maximizing routes for quantum networks, (2023).

[28] T. C. Ralph, A. J. F. Hayes, and A. Gilchrist, Loss-tolerant optical qubits, Phys. Rev. Lett. **95**, 100501 (2005).

[29] A. G. Fowler, D. S. Wang, C. D. Hill, T. D. Ladd, R. Van Meter, and L. C. L. Hollenberg, Surface code quantum communication, Phys. Rev. Lett. **104**, 180503 (2010).

[30] L. Jiang, J. M. Taylor, K. Nemoto, W. J. Munro, R. Van Meter, and M. D. Lukin, Quantum repeater with encoding, Phys. Rev. A , 032325 (2009).

[31] D. Gottesman, A. Kitaev, and J. Preskill, Encoding a qubit in an oscillator, Phys. Rev. A **64**, 012310 (2001).

[32] A. G. Fowler, D. S. Wang, C. H. Hill, T. D. Ladd, R. Van Meter, and C. L. Hollenberg, Surface code quantum communication, Phys. Rev. Lett. **104**, 180503 (2010).

[33] K. Azuma, K. Tamaki, and H. K. Lo, All-photonic quantum repeaters, Nat. Commun. **6**, 6787 (2015).

[34] S. Mulidharan, J. Kim, N. Lutkenhaus, M. D. Lucian, and L. Jiang, Ultrafast and fault-tolerant quantum communication across long distances, Phys. Rev. Lett. **112**, 250501 (2014).

[35] N. Lo Piparo, W. J. Munro, and K. Nemoto, Quantum aggregation with temporal delay, Phys. Rev. A **110**, 032613 (2024).

[36] Based on these observations, we generalize an aggregated path as a set of paths connecting two nodes with vary-

ing delays. Accordingly, we refine the definition of delay for such paths. For intuition, assume temporal delays are negligible, so delay depends only on path length. According to the protocol, if enough resources arrive via the shortest path, the receiver can decode the state immediately—yielding a delay equal to that of the shortest path. However, if additional resources are needed, decoding must wait for longer paths. Thus, the delay of an aggregated path is defined as the weighted average of the delays of all contributing paths, with weights given by the probability that each path successfully delivers sufficient resources.

[37] D. Bunandar, A. Lentine, C. Lee, H. Cai, C. M. Long, N. Boynton, N. Martinez, C. DeRose, C. Chen, M. Grein, A. Trotter, A. Starbuck, A. Pomerene, S. Hamilton, F. N. C. Wong, R. Camacho, P. Davids, J. Urayama, and D. Englund, Metropolitan quantum key distribution with silicon photonics, *Phys. Rev. X* **8**, 021009 (2018).

[38] S. J. Devitt, A. M. Stephens, W. J. Munro, and K. Nemoto, Requirements for fault-tolerant factoring on an atom-optics quantum computer, *Nature Communications* **4**, 2524 (2013).

[39] C. Panayi, M. Razavi, X. Ma, and N. Lutkenhaus, Memory-assisted measurement-device-independent quantum key distribution, *New J. Phys.* **16**, 043005 (2014).

[40] S. Zhou, M. Zhang, J. Preskill, and L. Jiang, Achieving the heisenberg limit in quantum metrology using quantum error correction, *Nat. Commun.* **9**, 78 (2018).

[41] S. Zhou, M. Zhang, J. Preskill, and L. Jiang, Achieving the heisenberg limit in quantum metrology using quantum error correction, *Nature Communications* **9**, 78 (2018).

[42] C. Elliott, Building the quantum network, *New J. Phys.* **4**, 46 (2002).

[43] B. Korzh, C. W. Lim, R. Houlmann, N. Gisin, L. M. J.,

D. Nolan, S. B., R. Thew, and Z. H., Provably secure and practical quantum key distribution over 307 km of optical fiber, *Nature Photonics* **9**, 163 (2015).

[44] R. Van Meter and D. Horsman, A blueprint for building a quantum computer, *Communications of the ACM* **10**, 83 (2013).

[45] M. Grassl, W. Geiselmann, and T. Beth, Loss-tolerant optical qubits, *International Symposium on Applied Algebra, Algebraic Algorithms, and Error-Correcting Codes*, , 231 (1999).

[46] I. F. Akyildiz, X. Wang, and W. Wang, Wireless mesh networks: A survey, *Computer Networks* **47**, 445 (2005).

[47] K. Liu and M. El Zarki, Qos routing in wireless ad hoc networks, *IEEE Network* **19**(3), 12 (2005).

Appendix A: Fidelities used in the unencoded case

Here we list the analytical expressions for the fidelities used to determine the curves in Fig. 4. We denote with F_{i+j} the fidelity of the corresponding $i+j$ configuration, in which i qudits are traveling in path 1 and j qudits are traveling in path 2.

$$\begin{aligned}
 F_{5+0} &= p_1^5. \\
 F_{4+1} &= p_1^4 p_2 \left[(1 - p_d)^4 + \frac{4}{7} p_d (1 - p_d)^3 \right. \\
 &\quad \left. + \frac{6}{7^2} p_d^2 (1 - p_d)^2 + \frac{4}{7^3} p_d^3 (1 - p_d) + p^4 / 7^4 \right]. \\
 F_{3+2} &= p_1^3 p_2^2 (1 - p_d)^3 + \frac{3}{7} p_d (1 - p_d)^2 \\
 &\quad + \frac{3}{7^2} p_d^2 (1 - p_d) + p^3 / 7^3]. \\
 F_{2+3} &= p_1^2 p_2^3 \left[(1 - p_d)^2 + \frac{2}{7} p_d (1 - p_d) + p^2 / 7^2 \right]. \\
 F_{1+4} &= p_1 p_2^4 [(1 - p_d) + p / 7]. \\
 F_{0+5} &= p_2^5.
 \end{aligned}$$